

Lawrence Berkeley National Laboratory

Recent Work

Title

PURITY OF CRYSTALS GROWN FROM BINARY ORGANIC MELTS

Permalink

<https://escholarship.org/uc/item/9130v68g>

Authors

Cheng, Cheng T.
Pigford, Robert L.

Publication Date

1969-11-01

PURITY OF CRYSTALS GROWN FROM BINARY ORGANIC MELTS

RECEIVED
LIBRARY
RADIATION LABORATORY

JAN 14 1970

Cheng T. Cheng and Robert L. Pigford

LIBRARY AND
DOCUMENTS SECTION

November 1969

AEC Contract No. W-7405-eng-48

TWO-WEEK LOAN COPY

*This is a Library Circulating Copy
which may be borrowed for two weeks.
For a personal retention copy, call
Tech. Info. Division, Ext. 5545*

LAWRENCE RADIATION LABORATORY
UNIVERSITY of CALIFORNIA BERKELEY

DISCLAIMER

This document was prepared as an account of work sponsored by the United States Government. While this document is believed to contain correct information, neither the United States Government nor any agency thereof, nor the Regents of the University of California, nor any of their employees, makes any warranty, express or implied, or assumes any legal responsibility for the accuracy, completeness, or usefulness of any information, apparatus, product, or process disclosed, or represents that its use would not infringe privately owned rights. Reference herein to any specific commercial product, process, or service by its trade name, trademark, manufacturer, or otherwise, does not necessarily constitute or imply its endorsement, recommendation, or favoring by the United States Government or any agency thereof, or the Regents of the University of California. The views and opinions of authors expressed herein do not necessarily state or reflect those of the United States Government or any agency thereof or the Regents of the University of California.

PURITY OF CRYSTALS GROWN FROM BINARY ORGANIC MELTS

Cheng T. Cheng* and Robert L. Pigford

Department of Chemical Engineering
and Lawrence Radiation Laboratory
University of California
Berkeley, California 94720

November 1969

ABSTRACT

Binary liquid mixtures of stilbene and bibenzyl form mixed crystals which, according to the phase diagram, should be considerably richer in stilbene than the liquid in which they grow. By watching the growth under a microscope using interference fringes to follow concentration changes, the solid phase composition can be determined as a function of growth rate and interface subcooling. The deviations from equilibrium are considerable. They are found to depend on the growth mechanism in accord with a theory following Eyring and Frank.

INTRODUCTION

The demand for ultrapure crystals in the solid state industry has stimulated extensive study of the processes by which crystals grow from the melt. The zone refining process, for example, has been very successful for producing pure metals but evidently has not yet been applied on a large scale in the organic chemical industry. The obvious need for improved continuous processes for the purification of high-melting organic compounds suggests that better understanding of the interface kinetic process itself--a key piece of information for rational design--is required.

* Present address: Engineering Technology Laboratory, Experimental Station,
E. I. duPont de Nemours and Co., Wilmington, Delaware

The process of crystal growth includes the diffusive transport of molecules from the bulk liquid to the interface, orientation of the molecules for attachment to the solid surface, and conduction of the latent heat of fusion from the interface. The resistance to diffusion and to heat conduction can be minimized easily by mechanical stirring but if the major resistance is in the interface itself stirring is of no help.

In zone refining studies the assumption of interfacial equilibrium has been used frequently as a boundary condition to solve the liquid phase mass transfer equation in order to obtain the distribution of the minor component. The slowness of the process may make this assumption acceptable in many cases. However, when the impurity content is large or when the process is to operate rapidly and especially when the phase diagram exhibits solid solution behavior the equilibrium assumption can hardly be justified. Under these conditions the separation effect owing to crystallization may be severely reduced owing to interface kinetics.

Most of the previous work on crystal growth rate phenomena has been confined to pure substances, the key relationship being that between the growth rate and the thermal undercooling of the melt (Van Hook, 1963, and Chalmers, 1964). Cahn, Hillig, and Sears (1964) reviewed such information with particular emphasis on the distinction between theories involving attachment of molecules to the whole of a microscopically flat crystal surface and those involving attachment to a few surface sites connected with dislocations. The use of assumption that the whole surface is effective has been criticized by Jackson *et. al.* (1967), who concluded that such theories can only be applied to second-order phase transitions.

Among the theories which involve surface defects there are several possibilities but a suggestion made originally by Frank (1948) has appeared to be the most promising for many substances. According to Frank, the surface imperfection to which liquid molecules are able to attach themselves is a self-perpetuating spiral defect consisting of a ledge step of molecular dimensions. Molecules can attach themselves in the corner of the step; as a result, the spiral winds around its center and eventually covers the whole crystal surface. Chernov (1961) has asserted that this screw dislocation mechanism, if it is not the only type of growth process, must be regarded as quite typical and universal.

THEORY OF THE GROWTH RATE OF A CRYSTAL FROM A SUBCOOLED BINARY MELTS

Following the usual assumption of Eyring (1941), the expression for the flux of component B toward the surface of a crystal to which both A and B molecules attach themselves is

$$N_B = f (\lambda_L k_L^F \rho_L y_B - \lambda_S k_S^R \rho_S x_B), \quad (1)$$

where the k 's represent forward and reverse first-order rate coefficients, respectively, and where $\rho_L y_B$ and $\rho_S x_B$ are the molar concentrations of B in the interfacial liquid and solid, respectively. The fraction of the interface surface which is available for the attachment of molecules coming from the liquid is f , which may be a small number if the interface structure contains very few vacancies. The λ 's represent the increments of distance accompanying the removal of one molecular spacing in the liquid or the addition of one layer of solid, respectively. If we assume that the lattice dimensions are inversely proportional to the molar densities we

may write Eq. (1) alternatively as

$$N_B = f \lambda_S \rho_S k_B^F \left(y_B - \frac{k_B^R}{k_B^F} x_B \right). \quad (2)$$

Since at equilibrium between the phases the flux must be zero we identify the ratio of the rate coefficients with the equilibrium phase compositions by

$$k_B^F/k_B^R = x_{Be}/y_{Be}, \quad (3)$$

which, in a binary system at constant pressure, is a function of the interface temperature only.

Completion of the theory requires that expressions be developed for one of the rate coefficients, following Eyring, and for the surface fraction, based on some assumption about the geometry of lattice imperfections at the interface. Before going into these steps, however, we first call attention to some aspects of the theory which appear to have escaped attention in the past.

If we define u_A as the average of the velocities of the A molecules as they move toward the surface we obtain

$$u_A = N_A/\rho_L y_A = f \lambda_L k_A^F \left(1 - \frac{y_{Ae} x_A}{x_{Ae} y_A} \right). \quad (4)$$

Similarly,

$$u_B = N_B/\rho_L y_B = f \lambda_L k_B^F \left(1 - \frac{y_{Be} x_B}{x_{Be} y_B} \right), \quad (5)$$

and in a binary system the two velocities are obviously related to each other. In fact, since each of the coefficients in front of the parenthesis is positive and since the parenthetical expressions in Eq. (4) and (5) must be of opposite sign, u_A and u_B can not both be positive. If B-molecules move toward the surface then A-molecules must move away from it, according to the equations.

This anomolous situation is easily resolved if one notes that each of the equations so far developed is true in a coordinate system which moves toward the interface at a velocity given by

$$u^* = y_A u_A + y_B u_B = f \lambda_L (k_A^F \Delta_A + k_B^F \Delta_B) . \quad (6)$$

In Eq. (6) the symbols Δ_A and Δ_B have been introduced as abbreviations for the driving forces,

$$\Delta_A = y_A - (y_{Ae}/x_{Ae})x_A \quad (7a)$$

$$\Delta_B = y_B - (y_{Be}/x_{Be})x_B . \quad (7b)$$

Obviously u^* can be positive, zero, or negative, depending on the ratio of the two forward rate constants.

Experimentally, it is difficult if not impossible to adjust the fluid velocity at the interface to the value u^* . In our experiments and in most others we have held the liquid-solid interface stationary and have measured the velocity, V , of the whole mass of liquid and solid needed to accomplish this. Thus, V is the velocity of propagation of the interface and the growth velocity of the crystal. The velocity of the liquid as it

approaches the stationary solid surface is not zero. A mass balance shows that the liquid moves at the velocity $V(\frac{\rho_S}{\rho_L})$ toward the interface, a value which can easily differ from u^* . Therefore, in order to obtain equations for the flux of each component in the laboratory coordinate system we must modify Eq. (1) by adding terms representing the convective transport of the components.

$$N_A = f \lambda_S \rho_S k_A^F \Delta_A + [V(\rho_S/\rho_L) - u^*] \rho_L y_A, \quad (8)$$

and a similar equation for N_B . By substituting u^* from Eq. (6) we obtain

$$N_A = f \lambda_S \rho_S (k_A^F \Delta_A y_B - k_B^F \Delta_B y_A) + V \rho_S y_A, \quad (9)$$

and

$$N_B = f \lambda_S \rho_S (k_B^F \Delta_B y_A - k_A^F \Delta_A y_B) + V \rho_S y_B. \quad (10)$$

It is not difficult now to obtain an equation for the composition of the solid which forms, for diffusion rates in the solid phase are so slow that the ratio of the mole fractions of the components is equal to the ratio of the molar fluxes onto the interface, i.e. $x_B = N_B/V \rho_S$, and Eq. (9) and (10) give

$$x_B = y_B + \frac{f \lambda_S}{V} (k_B^F \Delta_B y_A - k_A^F \Delta_A y_B), \quad (11)$$

and a similar equation for x_A . It is clear now that the difference in composition between solid and interfacial liquid depends on the growth rate

parameter, $\epsilon_B = f\lambda_S k_B^F/V$, and on the ratio of the two first-order coefficients. When the values of k^F are very large the parenthetical expression in Eq. (11) must be zero, which will require that both the Δ 's must be zero. Thus, phase equilibrium will be achieved. On the other hand, when the growth rate parameter is small the second term on the right will be negligible, despite a finite value for each of the Δ 's. Then $x_B = y_B$ and no enrichment of the crystal occurs as it grows, the composition of the solid being the same as that of the contiguous liquid.

An alternative method for expressing the result given in Eq. (11) has come into popular use in metallurgy and in zone refining technology. It is to define an "effective distribution coefficient" for each component as the ratio of the actual solid mole fraction to the mole fraction in the interface liquid: $K_B^* = x_B/y_B$ and $K_A^* = x_A/y_A$. These values may differ from the values based on the equilibrium phase diagram, $K_A = x_{Ae}/y_{Ae}$ and $K_B = x_{Be}/y_{Be}$, owing to the rate effects we have been discussing. From Eq. (11) we obtain

$$K_B^* = \frac{1 + (f\lambda_S k_B^F/V) \{ [1 - (k_A^F/k_B^F)] y_A + (k_A^F/k_B^F)(1/K_A) \}}{1 + (f\lambda_S k_B^F/V) \{ (y_A/K_B) + (k_A^F/k_B^F)(y_B/K_A) \}} \quad (12)$$

The equation for K_A^* is similar and can be obtained by exchanging subscripts in Eq. (12). According to Eq. (12), K_B^* approaches unity as the growth velocity increases or the forward rate constant decreases. As Eq. (12) indicates, the effective distribution coefficient, K^* , is not a constant, as has often been assumed; it depends on the temperature, the interfacial liquid composition and on the growth velocity. Its numerical value always lies between unity and the equilibrium value, K .

The result given by Eq. (11) can also be expressed in terms of the effective separation factor, defined by $\beta = (x_B/x_A)(y_A/y_B)$. This factor can be expected to be more nearly independent of composition than either K_A^* or K_B^* , at least for thermodynamically ideal systems. It is given by

$$\beta = \left(\frac{x_B}{x_A}\right)\left(\frac{y_A}{y_B}\right) = \frac{1 + (f\lambda_S k_B^F/V) \{ [1 - (k_A^F/k_B^F)] \cdot y_A + (k_A^F/k_B^F)(1/K_A) \}}{1 + (f\lambda_S k_B^F/V) \{ [(k_A^F/k_B^F) - 1] \cdot y_B + (1/K_B) \}} \quad (13)$$

In the limit of very large V , β approaches unity; there is no separation effect when the solid forms instantly in the liquid. At very small values of V , β approaches the value K_B/K_A .

ESTIMATION OF THE SURFACE STEP DENSITY, f

The surface step density, f , represents the fraction of the surface of the crystal which is available for attachment of individual molecules arriving from the liquid. For a surface that is sufficiently rough on a molecular scale, f is unity. According to Jackson (1967), many metals and some organic compounds which have very low values of the entropy of fusion are able to accept new atoms or molecules over their whole surfaces. For most substances, however, and particularly for more complex organic molecules only a very few positions on the crystal surface are available. The acceptable sites are in the corners of dislocation imperfections on the surface.

When a dislocation line intersects the crystal interface the dislocation winds itself into a screw as growth proceeds and provides a self-perpetuating spiral step into the corner of which new molecules can become

attached. According to Frank (1948) the spiral structure is approximately the shape of an Archimedean spiral having a constant spacing between adjacent branches that depends on the radius of curvature at the center of the spiral, r_c . Thus, the surface fraction for such a structure is equal to the ratio of the width of one molecule to the distance between branches of the spiral, or

$$f = \lambda/4\pi r_c . \quad (14)$$

Furthermore, if we assume that the size of the spiral at its center, where it has the smallest radius of curvature and the greatest ratio of surface to volume of any point along the spiral, is equal to the size of a two-dimensional nucleus which is just critically stable thermodynamically, we can equate r_c to $\sigma/\rho_S \Delta G$ where ΔG represents the difference of the Gibbs free energy of a mole of solid and a mole of liquid of the same composition and σ is the excess Gibbs free energy per unit of surface in the interface. Then the equation for f becomes

$$f = \lambda \rho_S \Delta G / 4\pi \sigma . \quad (15)$$

Using Turnbull's (1958) empirical expression for the surface energy,

$$\sigma = 0.3 \frac{\Delta H_f}{N^{1/3} V_S^{2/3}} , \quad (16)$$

where ΔH_f is the enthalpy of fusion and N is the Avagadro number, we get

$$f = \frac{1}{1.2\pi} \left(\frac{\Delta G}{\Delta H_f} \right) = \frac{1}{1.2\pi} \left(\frac{\Delta G}{T_m \Delta S_f} \right) . \quad (17)$$

Our expression for f must now be completed by an evaluation of the Gibbs free energy change, ΔG .

CHANGE IN GIBBS FREE ENERGY DURING SPONTANEOUS CRYSTAL GROWTH

If we have a pure melt from which the crystal is growing the free energy difference is very nearly equal to $\Delta S_f \Delta T$, where ΔT represents the difference between the equilibrium melting point and the interfacial temperature, i.e. the amount of subcooling. When the crystal is formed in a solution, however, the free energy change depends both on the composition of the liquid and on the interfacial temperature.

Consider first the formation of a pure crystal of compound B in a liquid mixture having interfacial mole fraction y_A of the "impurity" component, A. Then the chemical potential difference of B across the interface is given by Kirwan and Pigford (1969).

$$\Delta G = \mu_B^L - \mu_B^S = [\Delta S_f - \Delta C_{PB} \left(1 - \frac{T}{T_{Bm}}\right) - R \ln(\gamma_B y_B)] \Delta T , \quad (18)$$

where γ_B represents the activity coefficient of B in the interface liquid. The second term in the brackets is often negligible. Under these conditions the surface fraction f is somewhat reduced as compared with the value expected for crystallization from the pure liquid.

Moreover, for a system which forms a solid solution crystal, the thermodynamic driving force for growth can not be expressed simply in terms

of the interface subcooling, ΔT . As can be anticipated from Eq. (18), ΔG now depends both on interfacial temperature and on the interface composition driving forces.

The free energy change owing to phase transformation of one mole of liquid into one mole of solid solution, both liquid and solid having the solid's composition, is

$$\Delta G = (\mu_A^L - \mu_A^S)x_A + (\mu_B^L - \mu_B^S)x_B, \quad (19)$$

and the chemical potentials can be expressed in terms of their equal values on the liquidus and solidus curves of the phase diagram by the equations

$$\mu_B^L(y_B, T) = \mu_B^L(y_{Be}, T) + RT \ln(\gamma_B y_B / \gamma_{Be} y_{Be})$$

$$\mu_B^S(x_B, T) = \mu_B^S(x_{Be}, T) + RT \ln(\Gamma_B x_B / \Gamma_{Be} x_{Be}),$$

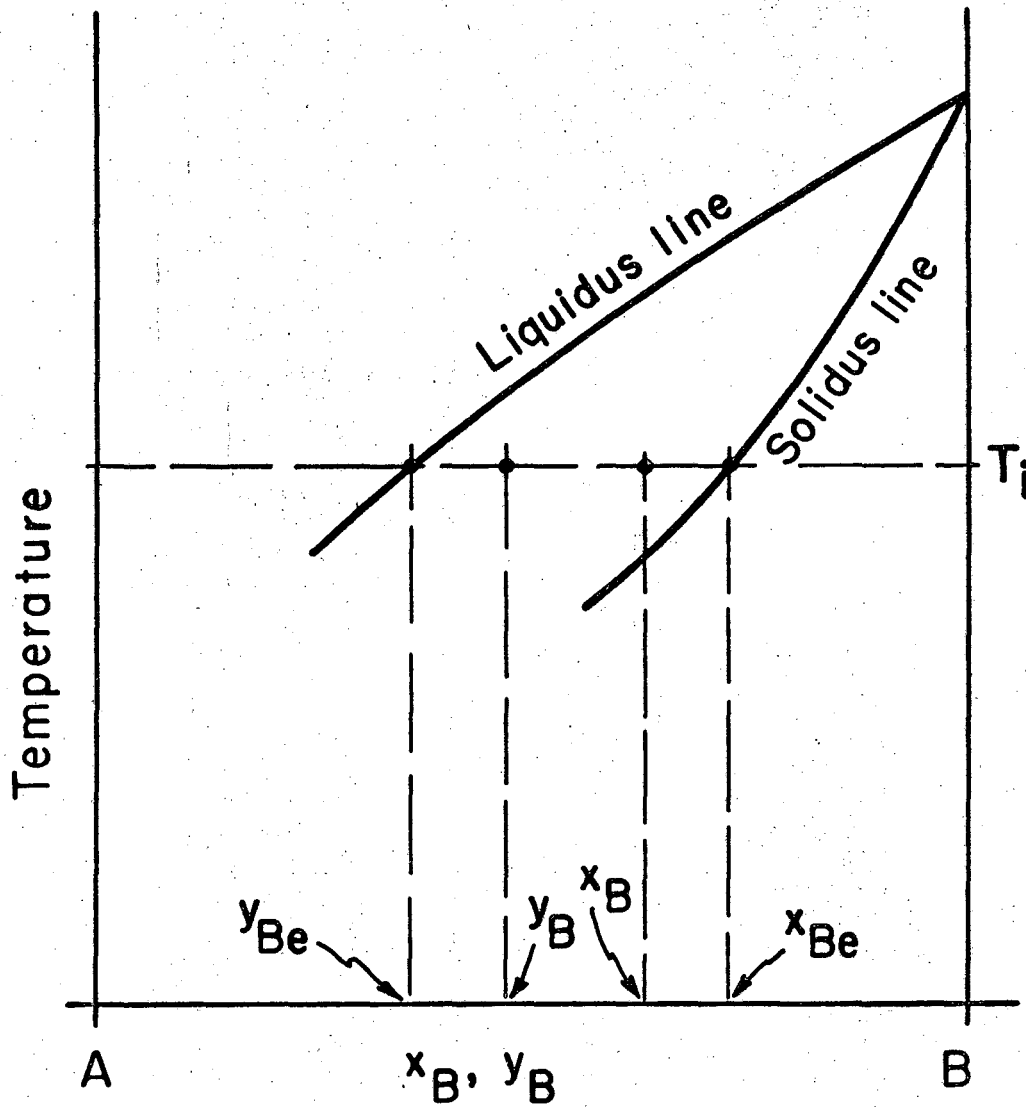
and two similar equations for component A. The γ 's represent activity coefficients in the liquid solution; Γ 's, in the solid solution. Substituting these expressions into Eq. (19) we get

$$\begin{aligned} \Delta G/RT = & x_A \ln(x_{Ae} y_A / y_{Ae} x_A) + x_B \ln(x_{Be} y_B / y_{Be} x_B) + x_A \ln(\gamma_A \Gamma_{Ae} / \gamma_{Ae} \Gamma_A) \\ & + x_B \ln(\gamma_B \Gamma_{Be} / \gamma_{Be} \Gamma_B). \end{aligned} \quad (20)$$

The first two terms represent the free energy changes if the liquid and solid solutions were ideal mixtures; the last two terms take care of

deviations from ideality. The activity coefficients can sometimes be obtained from the phase diagram without resorting to any assumptions about solution behavior. Note that temperature appears in this expression for ΔG through its effect upon the equilibrium mole fractions, y_{Be} , x_{Be} , etc. Note also that $\Delta G = 0$ when both the temperature and the compositions fall on the solidus and liquidus lines of the phase diagram. Presumably ΔG must be positive for the spontaneous growth process to occur. To bring these ideas out more clearly we refer to the hypothetical phase diagram in Fig. 1, which shows a possible location for the real and the equilibrium liquid and solid compositions at the observed interface temperature. Note that the liquid is cooled below its equilibrium freezing temperature on the liquidus curve and therefore has a greater free energy than at equilibrium; the solid, on the other hand, is at a temperature above its equilibrium melting point and is therefore superheated. It, too, has a greater free energy than it would have at equilibrium. The value of ΔG for the process of solidification is positive when the liquid is subcooled far enough and the solid is not superheated too far.

Some concern may be felt over the fact that the solid phase is indicated to be superheated, in view of the fact that all attempts to superheat solids above their melting points have proved fruitless. Note in connection with the present situation, however, that the solid is not only superheated but is also growing as a result of the continuous bombardment by molecules which come from the over-energetic liquid.



XBL6911-6182

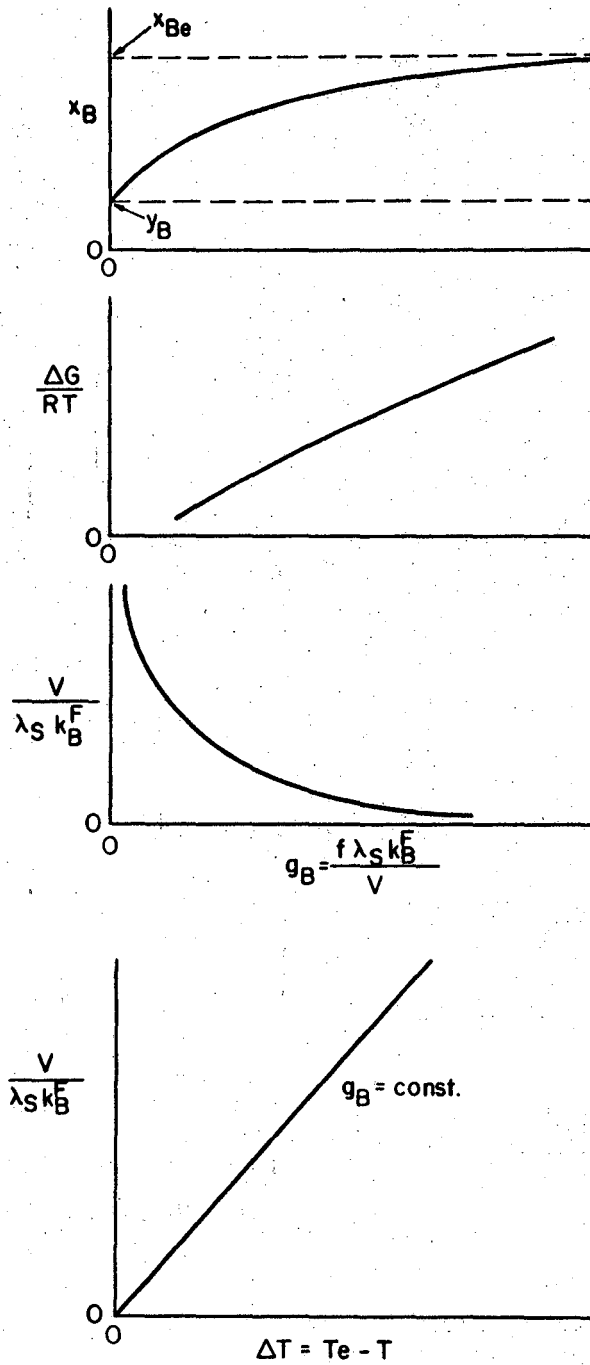
Fig. 1. Hypothetical phase diagram, bibenzyl and trans-stilbene system.

THE COMPUTATION OF THE CRYSTAL GROWTH VELOCITY, V

For a pure substance the crystal growth velocity is fixed when the temperature of the surrounding liquid is given; for growth from a binary solution fixing the interface temperature and the interface liquid composition are sufficient to determine V. How is such a relationship expressed by the equations given here?

From Eq. (12) one can compute the composition of the solid which forms in a liquid of fixed composition provided the ratio of the two forward rate constants (a function of temperature alone) is known and provided also that the group of variables, $f\lambda_S k_B^F/V$, is known. Thus for fixed T and y_B , x_B will be uniquely a function of $f\lambda_S k_B^F/V$. A typical relationship of this sort, computed for the binary system stilbene-bibenzyl, is shown in Fig. 2. As expected, the greater the value of the group the closer x_B approaches its equilibrium value at the assumed temperature.

Having found the solid composition it is now possible to compute ΔG and f, through Eq. (17). Furthermore, k_B^F is fixed by the temperature and is known. Thus, for each assumed value of the group, $f\lambda_S k_B^F/V$, all the quantities but V are determined, from which V follows by a simple computation. Fig. 2 also shows the relationship between ΔG and the dimensionless group for the illustrative example. By assuming $f\lambda_S k_B^F/V$ constant and varying y_B for fixed T it shows the values of $V/\lambda_S k_B^F$, which is proportional to f, is related to the undercooling, $\Delta T = T_e - T$, almost linearly as for pure compounds.



XBL6911-6179

Fig. 2. Relationship for the determination of mixed crystal growth velocity.

DETERMINATION OF THE RATE COEFFICIENTS, k_A^F and k_B^F

Following the method of Eyring (1941), the expression for the first-order rate coefficient is

$$k_B^F = \chi (kT/h) \exp(-\Delta G_C^\ddagger/RT) = \chi (kT/h) \exp(\Delta S_C^\ddagger/R) \exp(-\Delta H_C^\ddagger/RT), \quad (21)$$

and a similar expression for k_A^F . In Eq. (21) χ represents the fraction of the activated molecules which pass over the activation barrier in the direction. ΔG_C^\ddagger is the excess of the standard free energy of the molecule which is activated for crystallization over the value in the liquid, and ΔS_C^\ddagger and ΔH_C^\ddagger are the related entropy and enthalpy differences, respectively. Use of such an expression required a knowledge of the numerical values of these thermodynamic properties of the activated state for each substance in the mixture.

There is some reason to believe that, even though numerical values of the activation properties may not be available from direct measurement of crystal growth rates, values can be estimated by using the corresponding values derived from viscosity. Viscosities of liquids are far easier to measure experimentally than are growth velocities and the molecular mechanisms involved may be similar.

On the other hand, as pointed out by Kirwan and Pigford (1969), there are some differences in the molecular processes involved in crystal growth and in viscous flow. For instance, the molecule which approaches the crystal and becomes attached has to have the orientation that is required in the crystal lattice. The molecule which is ready to undergo viscous flow displacement may need to be oriented too, but the requirement

is not likely to be as stringent. Thus, it may be possible to estimate ΔS_C^\ddagger from ΔS_V^\ddagger by subtracting the entropy of fusion, ΔS_F from the latter, plus a small correction of R entropy units to account for the observation that perfectly spherical molecules undergo an entropy increase of R units upon melting. Moreover, there is reason to believe that the enthalpy of activation for crystallization may be smaller than that for viscosity (Kirwan and Pigford, 1969). To detach itself from its neighbor molecules in the liquid is all that is needed for crystal growth, but flow of a molecule also requires that a vacancy or hole be formed in the liquid at an adjacent site. Thus it may be that

$$\Delta H_C^\ddagger = c\Delta H_V^\ddagger, \quad (22)$$

where c is a constant probably smaller than unity. The best course of action, however, is not to try to compute ΔH_C^\ddagger unless no experimental crystallization data are available; a better plan is to make at least one measurement of the growth velocity and to determine the enthalpy of activation from that value, using it in Eq. (21) for estimates at other temperatures. Determination of both ΔS_C^\ddagger and ΔH_C^\ddagger from experimental data is not likely to be possible because it is unusual to be able to cover a wide enough range of temperatures in experimental work to give a reliable value of the slope of the curve of $\log(V)$ versus $1/T$.

EXPERIMENTAL RESULTS

Data were obtained for the binary system bibenzyl-stilbene, for which there is a wide range of solid compositions over which homogeneous

solid solutions are formed. The phase diagram for the system is shown in Fig. 3, based on the data of Kolosov (1958). The diagram shows that over most of the range of x the crystal structure resembles that of pure stilbene. At low mole fractions of stilbene there is a peritectic reaction but the compositions that were used in the experiments were all to the right of this range.

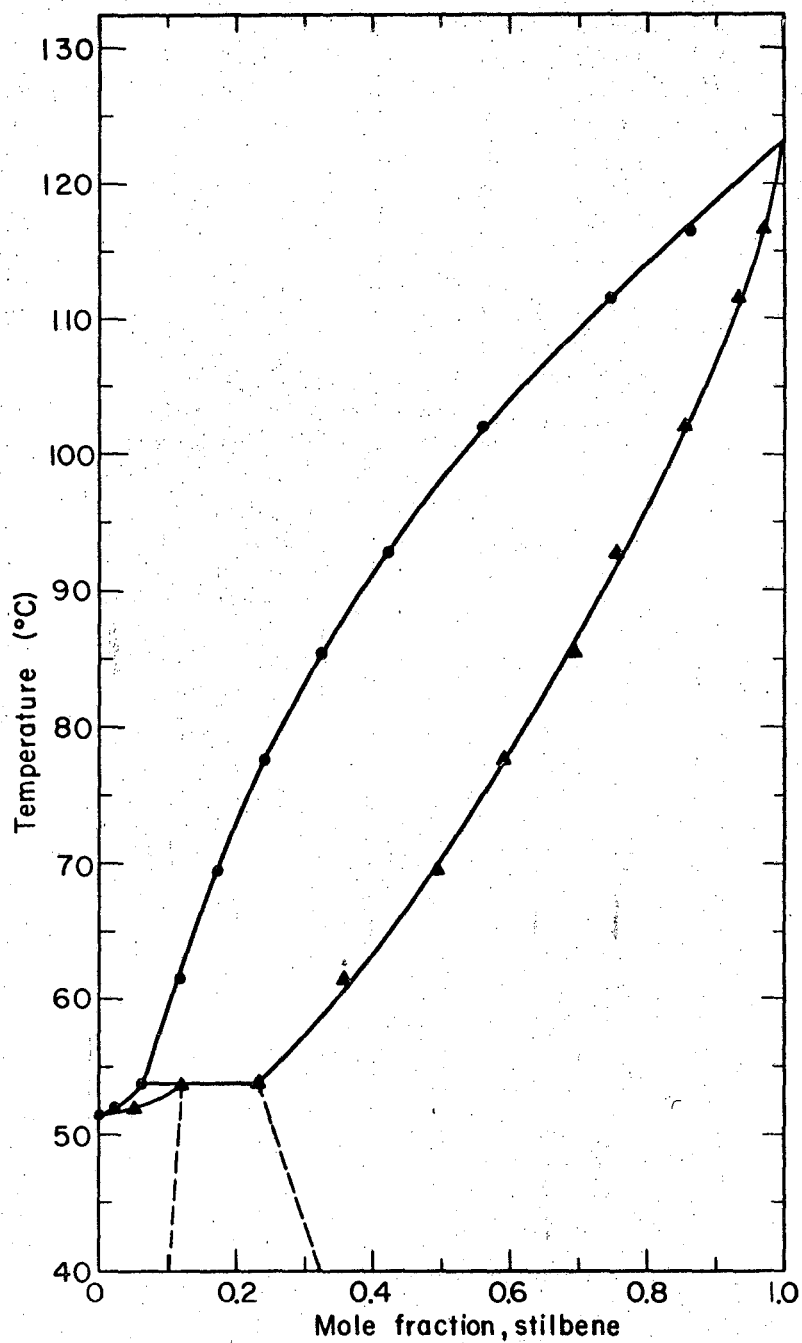
Crystallization rates and interfacial compositions and temperatures were observed with a temperature-gradient microscope stage, as described elsewhere (Cheng, 1969). The interface mole fraction of stilbene, y_B , was computed from the known composition of the liquid mixture introduced into the optical wedge of the apparatus and from the observed shift of the diffraction fringes owing to the concentration variation which accompanies the diffusion boundary layer in the liquid. The equation relating these quantities is

$$y_B = y_B^{(\infty)} - \Delta N(\lambda_0/2t)(\partial n/\partial y)_T^{-1}, \quad (23)$$

with ΔN = the number of fringe displacements at the interface, λ_0 = the wavelength of the laser light used, t = the wedge thickness at the observation point, and $(\partial n/\partial y)_T$ = the derivative of refractive index of the solution with respect to composition.

Compositions of the solid phase were determined in two ways. First, the same diffraction pattern was used in combination with a diffusion flux balance at the interface,

$$x_B = y_B + (\rho_L D/\rho_S V)(dy_B/dz)_{z=0}, \quad (24)$$



XBL6911-6190

Fig. 3. Phase diagram, bibenzyl and trans-stilbene system.

in which D is the binary diffusion coefficient in the liquid and dy_B/dz is the normal gradient of mole fraction at the interface. The latter quantity could be computed from careful measurements of the slopes of several diffraction lines using the equation

$$dy_B/dz = \frac{\lambda_0 S}{2 s t \cos \alpha (\sin \beta + S \cos \beta) (\partial n / \partial y)_T} \quad (25)$$

where S represents the measured slope of the diffraction fringes and s is their spacing. The angles α and β represent inclinations of the crystal face and of the distant straight diffraction lines, respectively. A detailed derivation of these equations is given elsewhere (Cheng, 1969).

In order to obtain an independent check of the computed solid compositions, a few measurements were obtained by taking small samples of the solid phase obtained from the diffraction wedge and subjecting these to ultra violet absorption analysis in ethanol. Such measurements were tedious and somewhat inaccurate but they agreed fairly well with the computed compositions using Eqs. (23) and (24), as will be seen shortly.

The pure materials were carefully purified by zone refining and sublimation. Measured melting points of the purified samples were 123.0°C for trans-stilbene (vs. 123.3°C reported (Kolosov, 1958)) and 52.03°C for bibenzyl (vs. 51.1°C reported (Kolosov, 1958)). Other properties of the pure components are shown in Table I.

The liquid diffusion coefficient was not measured directly. A value observed by Kirwan (1967) was combined with an estimate based on the empirical correlation of Wilke and Chang (1955); the value used was

7.6×10^{-6} sq. cm/sec at 63.3° C. It is believed to have a probable uncertainty of about $\pm 20\%$. The intermolecular spacing for the solid, λ_s , was computed by taking the cube root of the column of the solid phase per molecule. Liquid viscosity data were determined by Kirwan (1967).

Table I. Physical Properties of Pure Materials^a

Substance	M.W.	T _m	ΔH_f	ΔS_f	$\sigma \times 10^7$	η	ΔH_V^\ddagger	ΔS_V^\ddagger
		$^\circ\text{K}$	cal/g mole		(cal/cm ²)	c.p.	cal/g mole	
Bibenzyl	182.27	325.18	5580	17.18	4.76	2.0	3243	-3.709
t-stilbene	180.25	396.15	7080	17.87	8.70	1.0	3625	-3.083

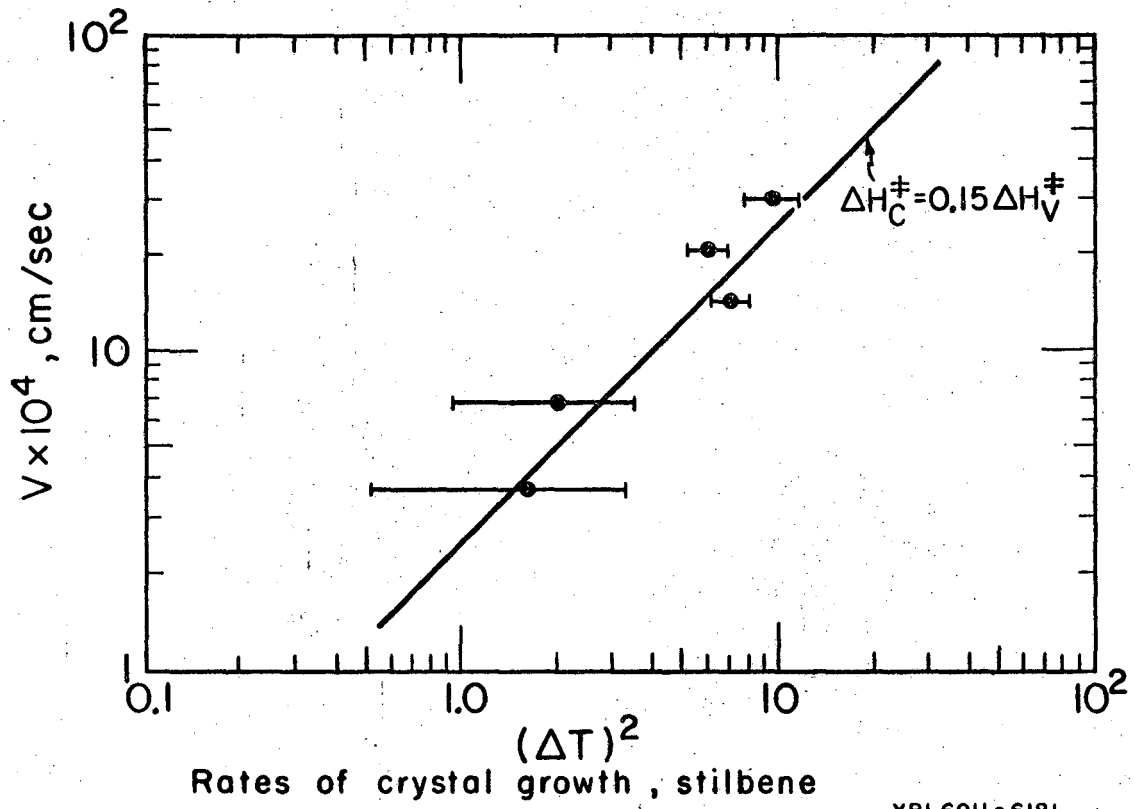
^aDimensions see notation

DATA FOR PURE STILBENE

Figure 4 shows the experimentally observed growth velocities for pure trans-stilbene. The data are plotted in the form V vs. the square of the undercooling, ΔT . It can be shown that for the screw dislocation surface mechanism and for values of $\Delta S_f \Delta T / RT_m$ that are sufficiently small.

Equating the average velocity of movement toward the surface of the B molecules to the fluid velocity toward the same surface, $V(\rho_S/\rho_L)$, we get

$$V = f \lambda_S k_B^F \Delta_B = f \lambda_S k_B^F \left[1 - \exp\left(-\frac{\Delta S_f \Delta T}{RT}\right) \right]$$



XBL6911-6181

Fig. 4

or

$$\begin{aligned}
 V &\sim (1/1.2\pi)(\lambda_S k_B^F)(\Delta S_f \Delta T / \Delta H_f)(\Delta S_f \Delta T / RT_m) \\
 &= (1/1.2\pi)(\lambda_S k_B^F)(\Delta S_f / R)(\Delta T / T_m)^2, \quad (26)
 \end{aligned}$$

in which the exponential term has been expanded in a series. The data on the figure are not sufficiently accurate, owing to uncertainties in the interface temperature, to test the hypothesis that V is proportional to the square of ΔT . However, if we evaluate the entropy of activation in k_B^F from the equation,

$$\Delta S_C^\ddagger = \Delta S_V^\ddagger - (\Delta S_f - R), \quad (27)$$

and approximate the enthalpy of activation by choosing $c = 0.15$ in Eq. (22) we obtain a line from Eq. (26) which passes through the data points. In view of the reasonable values of the activation quantities and the at least approximate agreement of the exponent on ΔT with the expected value, it seems likely that the pure stilbene crystals grew by the screw dislocation mechanism.

Evaluation of the surface fraction leads to $f \sim 6 \times 10^{-4}$ for stilbene at one degree of subcooling.

DATA FOR STILBENE-BIBENZYL SOLUTIONS

The experimental data for interface liquid and solid compositions and interfacial liquid temperatures are listed in Table II for three series of runs, each series corresponding to a constant value of the liquid mole

fraction of stilbene at a great distance from the crystal, y_{B0} . The observed liquid and solid compositions are plotted in Fig. 5. There one sees that, owing to the finite growth velocity, the interfacial liquid mole fraction of stilbene fell slightly below y_{B0} at finite values of V . The greatest deviation from equilibrium occurred in the solid composition, as shown by the upper lines in the figure. At very small values of V the values of x_B tended toward the equilibrium value but at most of the values of V used x_B fell considerably below its equilibrium value. At large values of V the crystal's composition differed only very slightly from that of the liquid from which it grew. The figure shows that the principal cause of the failure to reach equilibrium was not the diffusional resistance of the liquid but the slowness of phase growth.

Although the measurements were carried out with great care it is of course possible that the solid compositions which were obtained by calculation from the diffusion flux balance, Eq. (24), were in error. This could have occurred if any of the measurements were not precise, if the estimated diffusion coefficient was wrong, or if the growing crystals did not fill the optical wedge completely. By computation of the possible errors of measurement it was concluded that the true value of y_B might have been off by about 0.0042 mole fraction and that the derivative, dy_B/dz might be in error by about 0.0052 mole fraction units. The probable error of D was estimated to be about 20 percent. The other quantities in the equation were precise. Thus, the total probable error in x_B should have been about 0.01 mole fraction units, which is smaller than the vertical difference between the pairs of curves on Fig. 5.

Table II. Crystallization of Mixed Crystals from Binary Melts of Stilbene and Bibenzyl System

Run No.	V , (cm/sec) $\times 10^3$	$y_B(0)$, mole fraction	$x_B(0)$, mole fraction	$T(0)$, $^{\circ}\text{C}$	T_e^a , $^{\circ}\text{C}$	y_{Be} , mole fraction	x_{Be} , mole fraction	$x_{B,cal}^b$
$y_{B0} = y_B(\infty) = 0.15$ mole fraction, stilbene								
III- 72	0.68	0.1356	0.1498	63.53	64.22	0.131	0.397	0.150
III- 73	1.00	0.1319	0.1411	64.17	63.70	0.135	0.407	c
III- 75	1.92	0.1388	0.1437	62.11	64.67	0.120	0.374	0.157
III- 76	0.51	0.1263	0.1671	63.61	62.93	0.131	0.398	c
III- 77	0.50	0.1407	0.1585	63.08	64.97	0.127	0.390	0.189
III- 99	0.74	0.1273	0.1513	63.37	63.07	0.129	0.394	c
III-101	0.34	0.1295	0.1707	62.86	63.38	0.126	0.386	0.150
III-102	0.40	0.1370	0.1662	62.68	64.41	0.125	0.383	0.190
III-103	0.15	0.1365	0.2055	62.48	64.35	0.123	0.380	0.249
III-104	0.13	0.1397	0.2224	63.17	64.78	0.128	0.391	0.252
III-105	0.39	0.1415	0.1702	62.73	65.04	0.125	0.384	0.210
III-106	0.21	0.1452	0.1784	61.82	65.53	0.118	0.370	0.281
III-107	0.31	0.1436	0.1736	63.28	65.32	0.129	0.393	0.220
III-140	0.42	0.1436	0.1651	63.65	65.32	0.131	0.399	0.196
III-141	0.35	0.1358	0.1624	62.49	64.19	0.123	0.380	0.189
III-143	0.23	0.1401	0.1760	63.76	64.84	0.132	0.400	0.198
III-144	0.15	0.1410	0.2019	63.06	64.98	0.127	0.389	0.258
III-145	0.09	0.1461	0.1923	63.49	65.66	0.130	0.396	0.307
III-146	0.03	0.1445	0.3168	62.13	65.44	0.121	0.375	0.381

(continued)

Table II. continued

Run No.	V	$y_B(0)$	$x_B(0)$	T(0)	T_e^a	y_{Be}	x_{Be}	$x_{B,cal}^b$
	(cm/sec) $\times 10^3$	mole fraction		$^{\circ}C$	$^{\circ}C$	mole fraction		
$y_{B0} = y_B(\infty) = 0.15$ mole fraction, stilbene								
III-147	0.20	0.1371	0.1973	62.66	64.43	0.124	0.383	0.225
III-148	0.73	0.1466	0.1519	60.10	65.73	0.106	0.342	0.228
III-149	0.25	0.1398	0.1864	62.22	64.80	0.121	0.376	0.240
IV - 1	0.21	0.1428	0.1907	63.13	65.21	0.128	0.391	0.243
IV - 2	0.15	0.1425	0.2123	63.94	65.16	0.134	0.403	0.232
IV - 3	0.10	0.1431	0.2483	62.93	65.25	0.126	0.387	0.301
IV - 4	0.07	0.1424	0.2801	63.12	65.15	0.128	0.390	0.313
IV - 5	0.79	0.1429	0.1508	64.86	65.23	0.140	0.417	0.150
IV - 6	0.65	0.1404	0.1542	62.90	64.89	0.126	0.387	0.180
IV - 7	0.35	0.1381	0.1616	62.37	64.57	0.122	0.379	0.208
IV - 8	0.15	0.1417	0.2014	62.74	65.08	0.125	0.384	0.271
IV - 9	0.24	0.1459	0.1647	63.64	65.63	0.131	0.399	0.237
IV - 10	0.12	0.1416	0.2256	63.42	65.08	0.130	0.395	0.261
$y_{B0} = y_B(\infty) = 0.25$ mole fraction, stilbene								
III- 78	0.48	0.2314	0.2623	74.04	76.33	0.212	0.548	0.333
III- 79	0.87	0.2307	0.2494	75.86	76.25	0.227	0.571	0.244
III- 80	1.33	0.2271	0.2364	74.77	76.84	0.218	0.557	0.269
III- 81	1.62	0.2353	0.2411	74.36	76.77	0.215	0.552	0.276

(continued)

Table II. continued

Run No.	V , (cm/sec) $\times 10^3$	$y_B(0)$, mole fraction	$x_B(0)$, mole fraction	T(0) , $^{\circ}\text{C}$	T_e^a , $^{\circ}\text{C}$	y_{Be} , mole fraction	x_{Be} , mole fraction	$x_{B,cal}^b$,
$y_{B0} = y_B(\infty) = 0.25$ mole fraction, stilbene								
III- 84	0.16	0.2327	0.3257	75.56	76.48	0.225	0.568	0.350
III- 85	0.52	0.2404	0.2574	75.03	77.42	0.220	0.561	0.344
III- 86	1.24	0.2357	0.2486	75.13	76.81	0.221	0.562	0.274
III- 89	0.89	0.2276	0.2452	74.83	75.89	0.219	0.558	0.260
III- 91	2.00	0.2392	0.2450	74.26	77.22	0.214	0.550	0.280
III- 92	0.71	0.2247	0.2474	74.80	75.56	0.218	0.558	0.254
III- 93	0.96	0.2297	0.2439	74.34	76.13	0.214	0.552	0.278
III- 94	0.57	0.2330	0.2505	74.26	76.51	0.214	0.550	0.323
III- 96	0.10	0.2345	0.3953	76.42	76.68	0.232	0.579	0.301
III- 97	0.06	0.2377	0.5202	76.42	77.04	0.232	0.579	0.411
III- 98	0.13	0.2368	0.3842	74.90	76.94	0.219	0.559	0.442
$y_{B0} = y_B(\infty) = 0.45$ mole fraction, stilbene								
III-108	0.83	0.4350	0.4546	92.74	93.88	0.419	0.762	0.506
III-109	0.58	0.4356	0.4685	93.88	93.93	0.435	0.774	0.441
III-110	0.39	0.4412	0.4790	92.59	94.33	0.417	0.761	0.597
III-113	0.16	0.4436	0.5000	91.37	94.50	0.401	0.749	0.707
III-115	0.76	0.4308	0.4646	91.17	93.58	0.399	0.746	0.556
III-116	0.34	0.4398	0.4934	92.75	94.23	0.420	0.763	0.594

(continued)

Table II. continued

Run No.	V , (cm/sec) $\times 10^3$	$y_B(0)$, mole fraction	$x_B(0)$, mole fraction	T(0) , $^{\circ}\text{C}$	T_e^a , $^{\circ}\text{C}$	y_{Be} , mole fraction	x_{Be} , mole fraction	$x_{B,cal}^b$,
$y_{B0} = y_B(\infty) = 0.45$ mole fraction, stilbene								
III-117	0.29	0.4427	0.4946	93.00	94.44	0.423	0.765	0.609
III-118	0.15	0.440	0.5795	93.38	94.53	0.428	0.769	0.645
III-119	0.14	0.4309	0.5815	90.32	93.59	0.388	0.738	0.704
III-132	0.86	0.4318	0.4678	87.55 ^d	93.65	0.353	0.708 ^d	0.616 ^d
III-133	0.47	0.4276	0.4784	95.63	93.34	0.460	0.791	c
III-134	0.72	0.4412	0.4648	93.23	94.33	0.426	0.767	0.519
III-135	2.08	0.4412	0.4470	92.96	94.33	0.422	0.765	0.480
III-136	2.99	0.4428	0.4471	91.19	94.45	0.399	0.747	0.500
III-137	1.49	0.4388	0.4485	92.39	94.16	0.415	0.759	0.502
III-138	2.06	0.4361	0.4443	91.90	93.97	0.408	0.754	0.490
III-139	0.45	0.4318	0.4704	95.62	93.65	0.459	0.791	c

^a Equilibrium temperature based on interfacial composition, $y_B(0)$.

^b With k_B^F calculated from Eq. (21) using $\chi = 0.01$, and $\Delta T = T_e - T(0)$ for computing step density f .

^c Because of negative ΔT , this value is not computed.

^d Measured interfacial temperature $T(0)$ was in error.

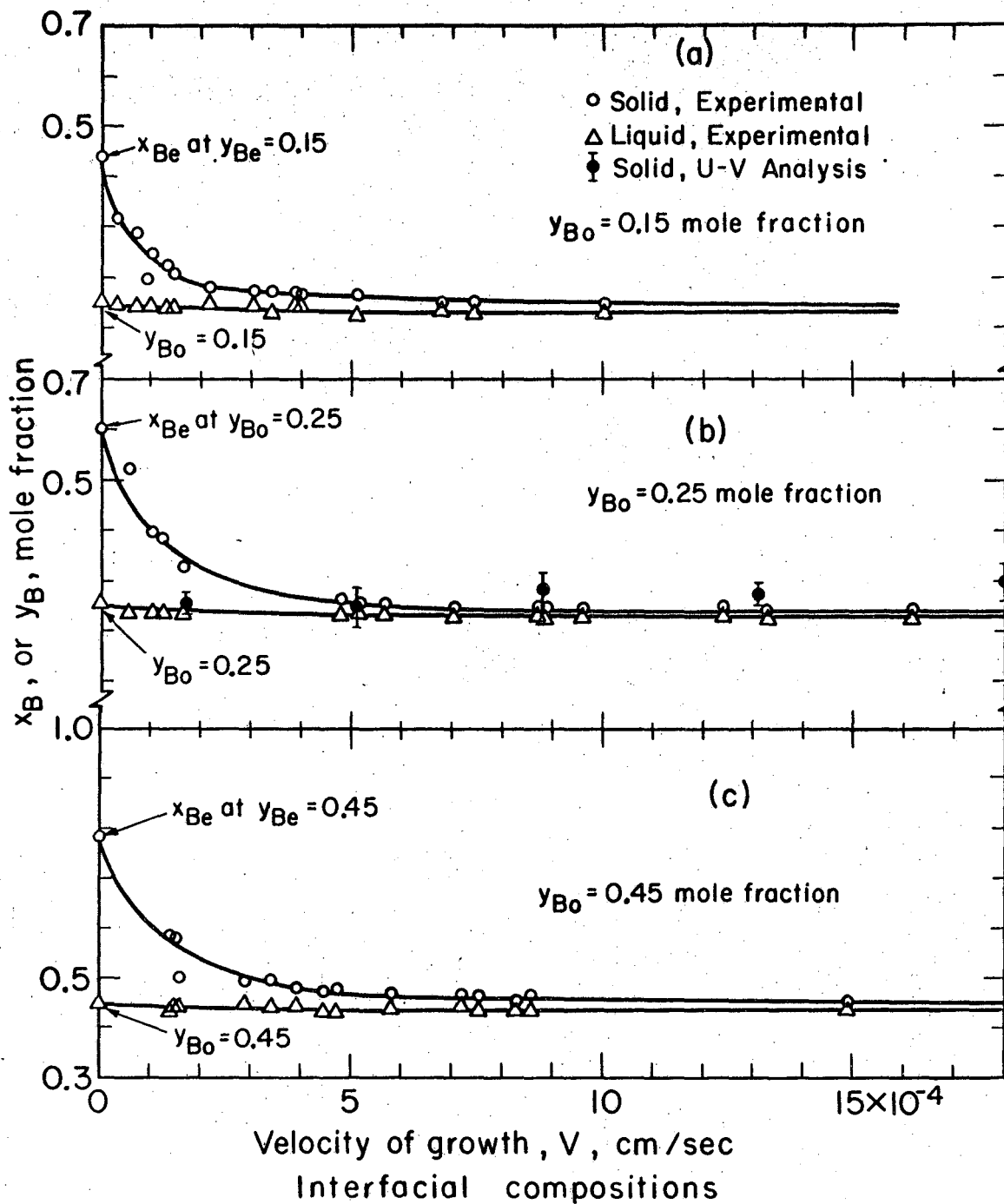


Fig. 5. Interfacial compositions, bibenzyl and trans-stilbene system.

An even stronger indication that the measured values of x_B are reliable was obtained when some of the crystallization runs were repeated and small samples of the solid were taken from the optical wedge and analyzed by ultra violet absorption. The following table summarized the values obtained and supports the use of Eq. (24). The results of such analyses are also shown in Fig. 5.

Table III. Comparison of Solid Compositions Computed from Flux Balance with Values from Ultra Violet Absorption

Growth Velocity $V \times 10^3$, cm/sec	Mole Fraction Stilbene, x_B	
	From Eq. (24)	From Ultra Violet Analysis
1.85	0.240 ± 0.010	0.300 ± 0.031
1.31	0.243 ± 0.010	0.274 ± 0.019
0.88	0.251 ± 0.010	0.284 ± 0.033
0.51	0.260 ± 0.015	0.248 ± 0.039
0.17	0.340 ± 0.015	0.252 ± 0.017

One other piece of evidence is available to support the reported values of x_B . It consists of the measurements, also using Eq. (24), of the composition of the solid phase which grows at a finite rate in the system of salol-thymol. These compounds are completely insoluble in each other as solids, the phase diagram indicating that to the right of the eutectic point, $x_{Be} = 1$ and $x_{Ae} = 0$. Application of Eq. (11) shows that the rate theory is satisfied under these conditions only by the value $x_A = 0$ at finite V . Compute values of x_A based on the diffraction fringes, were not precisely zero but were close. The average value for several experiments

was about 0.1. Recognize, however, that the theory which we have used may be defective in such a situation for it assumes that the surface fraction for attachment of A molecules and that for B molecules is exactly the same. In fact, it may be possible that f_A is zero on a pure-B surface.

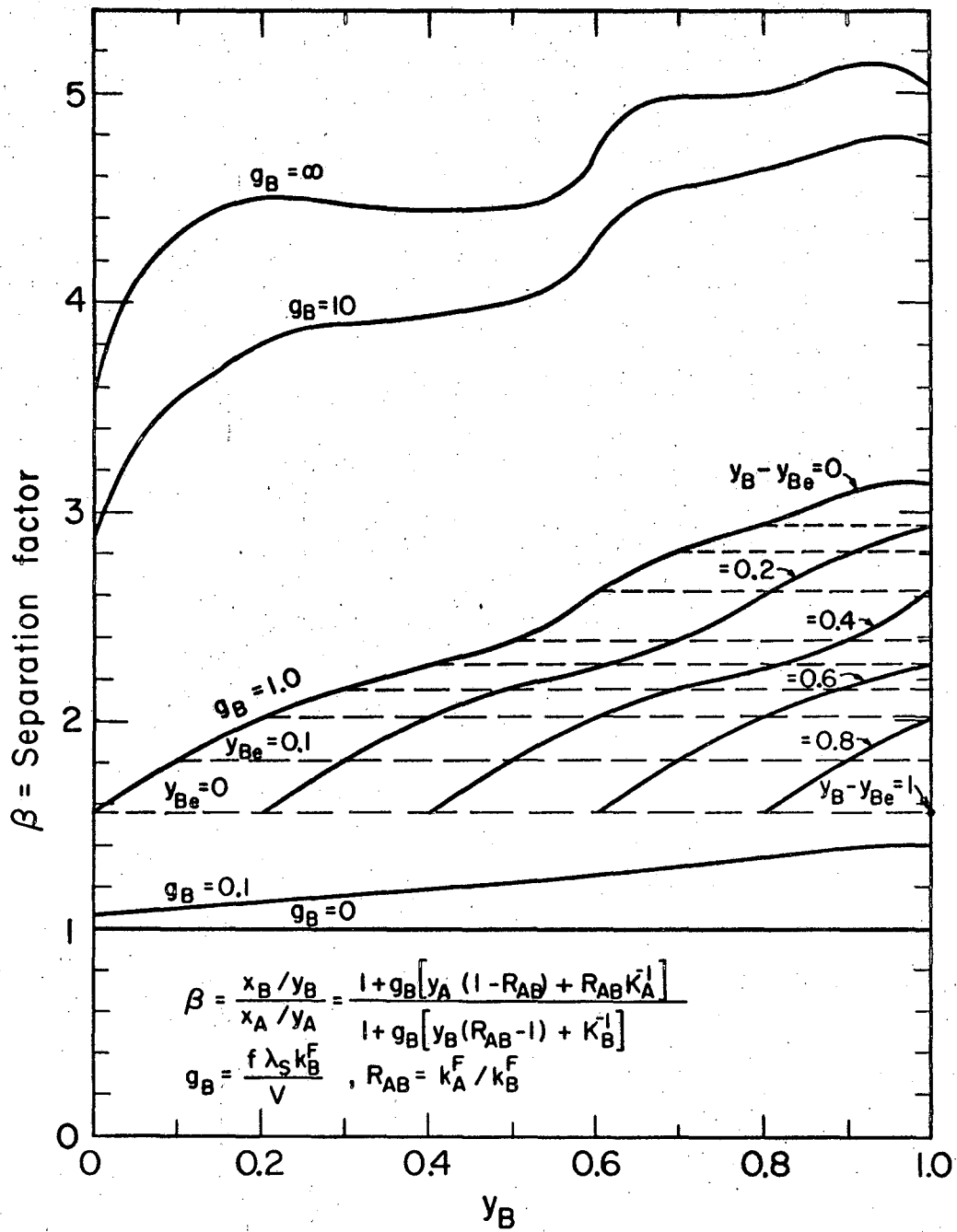
INTERPRETATION OF THE RESULTS

The Separation Factor, β : Figure 6 shows values of the separation factor based on Eq. (13) using the thermodynamic properties of the stilbene-bibenzyl system and assuming $c = 0.15$ in Eq. (22). The dimensionless quantity $g_B = f\lambda_S k_B^F/V$ is sufficient to determine β as a function of the interface composition and temperature. As g_B increases the equilibrium separation factor is approached. Figure 7 compares the separation factors computed from the observed compositions with values found from Fig. 6. Some of the data points are based on $c = 1.0$; others, on $c = 0.15$. The difference is small because only the ratio of the two forward coefficients, k_A^F/k_B^F , is affected in the rate theory. The agreement is satisfactory.

Determination of the Surface Step Density and the Rate

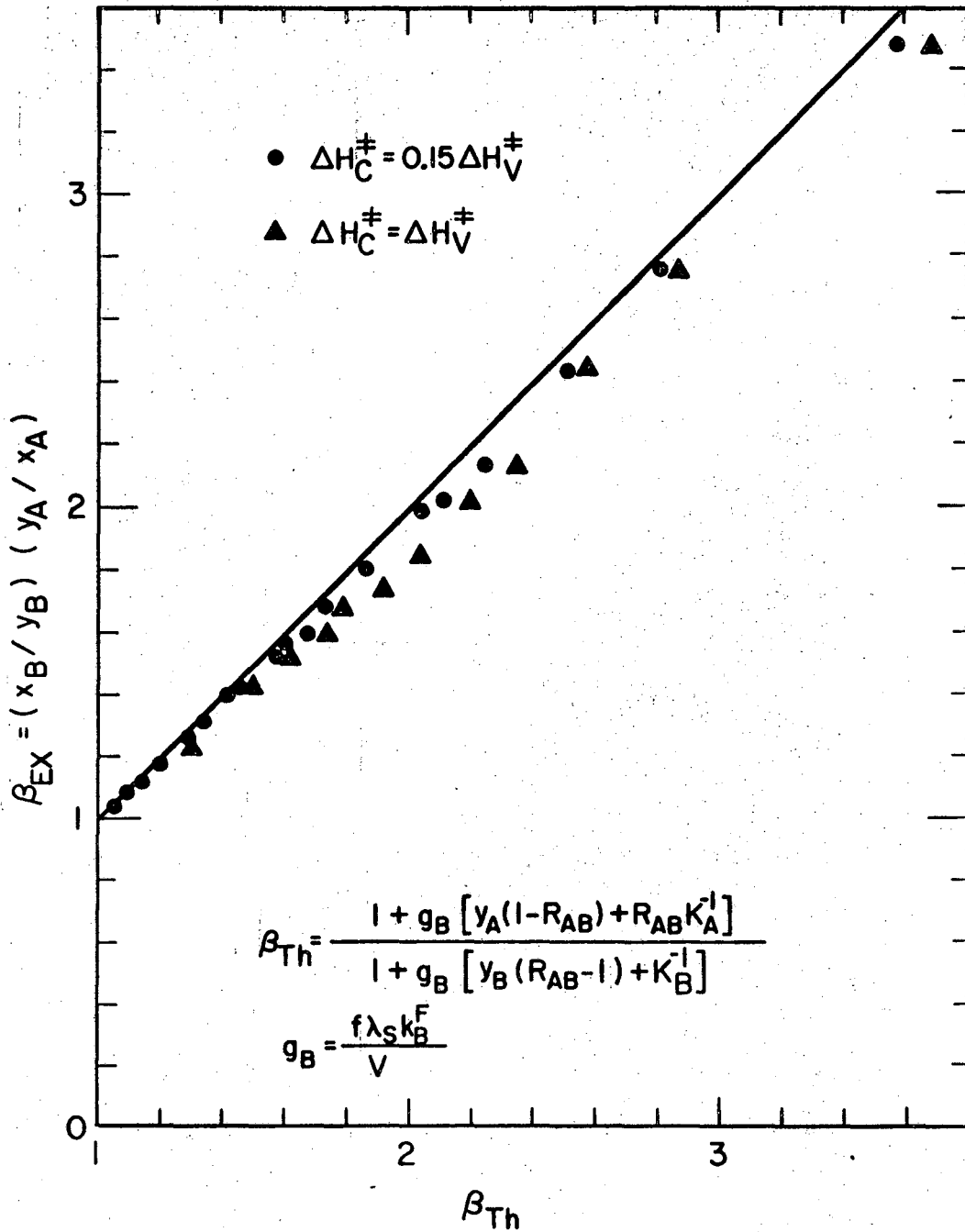
Coefficient: Using the observed solid and interfacial liquid compositions and temperature and the crystal growth velocity it is possible to compute values of the product $f k_B^F$ from Eq. (11). The determination of the separate values of f and k_B^F is not possible; one has to be found from the theory in order to determine the other from the data.

There are two ways in which the surface fraction, f , can be determined from the experimentally observed interface temperature, and the interface liquid and solid compositions. First, the values of V , T , y_B , and



XBL6911-6189

Fig. 6. Separation factor, bibenzyl and trans-stilbene system.



XBL6911-6178

Fig. 7. Comparison of separation factors, bibenzyl and trans-stilbene system.

x_B can be substituted in Eq. (11) to obtain values of the group $f\lambda_S k_B^F$. Then with estimates of λ_S and of k_B^F and k_A^F (the latter from the Eyring theory, Eq. (21), and ΔS_C^\ddagger and ΔH_C^\ddagger from Eq. (27) and (22) with $c = 0.15$) f follows directly, provided χ is known. Assuming $\chi = 1$ yields $f \approx 10^{-5}$, which is about two orders of magnitude greater than the value obtained from the data for pure stilbene. Thus, in order to reconcile the data for the pure crystal with those for the solution one may assume $\chi \approx 10^{-2}$.

Alternatively, f can be computed from Eq. (17) using values of ΔG found from the compositions and temperatures using Eq. (20) and, in the absence of any data, assuming ideal solution behavior in both the solid and the liquid phases. According to such calculations, ΔG was negative for all but two of the experimental runs--a situation which is manifestly impossible since it implies that the spontaneous process of phase growth occurs with an increase in the Gibbs free energy of the material forming the crystal surface.

It seems very possible that in a system which exhibits peritectic phase behavior over some part of the composition range there will be deviations from ideal solution behavior throughout the phase diagram and that the values of chemical potential estimated by assuming that γ and Γ are both unity will be erroneous. No data are available to test this belief but, in order to determine how sensitive the computations might be to small deviations in ideality the regular-solution equation for activity coefficients was introduced:

$$\ln \gamma_B = (\omega^L/RT) y_A^2 \quad (\text{liquid phase})$$

$$\ln \Gamma_B = (\omega^S/RT) x_A^2 \quad (\text{solid phase})$$

The result of adding the non-ideal terms to Eq. (20) is to increase the value of $\Delta G/RT$ by the quantity

$$(\omega^S/RT)(x_{Be} - x_B)^2 - 2(\omega^L/RT)(y_B - y_{Be})(x_B - \frac{y_B + y_{Be}}{2}) .$$

The first term, reflecting the influence of non-ideal behavior in the solid phase, has a positive coefficient; the coefficient of the second term is negative. In a typical experiment, Run No. III-93 of Table II, the expression above is $-0.0007(\omega^L/RT) + 0.095(\omega^S/RT)$ and the uncorrected ideal value of $\Delta G/RT$ based on the observed liquid and solid compositions and the temperature was -0.359 . The coefficient of (ω^L/RT) is small because the interface liquid composition was rather close to the equilibrium value; the coefficient of (ω^S/RT) is larger because x_B was considerably less than x_{Be} . Since ω^L is likely to be smaller than ω^S it seems likely that the term representing the lack of ideality in the liquid can be neglected completely and that we can conclude that (ω^S/RT) must have been at least $0.359/0.095 = 3.78$ or $\omega^S = 2.5$ kcal/mole in order to force the change in Gibbs free energy negative for the transition from liquid to solid.

In the absence of reliable thermodynamic information for the solid solution we can only conclude that the experimentally observed compositions probably do not violate the Second Law. When the information is available it will be possible to recalculate the values of ΔG and to estimate the

surface fraction f from the assumption of growth by a screw dislocation mechanism. In the mean time we have no reason to doubt the validity of Eq. (11) for the solid composition or of Eq. (17) for the surface fraction.

Table II shows values of the solid composition, x_B , computed from the theory using $\chi = 0.01$ and taking the activation quantities from viscosity with modifications according to Eq. (21) and (22) with $c = 0.15$. The values are by no means in perfect agreement with those observed but the departure from equilibrium is of the right magnitude and the variation with the growth velocity is about right. When no experimental information whatever is available this procedure is suggested.

CONCLUSIONS

Use of the temperature-gradient microscope stage with provisions for determination of interface conditions by optical interference is a promising method for investigating the interfacial kinetic phenomena. For the binary system used here and probably for most other high-melting organic compounds which form solid solutions the interfacial rate of phase growth is the controlling factor in the determination of the solid composition; the diffusion process in the interfacial liquid is of minor importance.

A theory based on Eyring's theory for the first-order process of solid deposition and on a screw-dislocation mechanism for surface attachment accounts approximately for the observed phenomena, including the large departure of the solid composition from its equilibrium value according to the phase diagram. In the absence of any experimental rate data, estimates of the interfacial rate coefficients can be based on activation enthalpy and viscosity from viscosity data suitably adjusted to account for differences in the molecular phenomena accompanying crystal growth and viscous flow.

ACKNOWLEDGMENTS

These studies were supported by AEC Contract w-7405-eng-48. The authors express their thanks to the Atomic Energy Commission for its support. Ray G. Clem of the Lawrence Radiation Laboratory performed the ultra violet analysis for the solid composition.

NOTATION

- C_p = molar heat capacity, cal/g mole °C
- D = diffusion coefficient, or interface transport coefficient, sq cm/sec
- f = surface step density, dimensionless
- g_B = dimensionless growth rate parameter, $\lambda_S f k_B^F / V$
- G = molar free energy, cal/g mole
- h = Planck's constant
- H = molar enthalpy, cal/g mole
- k = interfacial rate constant, sec^{-1} , or Boltzmann's constant, erg/°K
- K = equilibrium or effective distribution coefficient, a function of composition
- M = molecular weight
- n = refractive index of liquid
- N = crystallization flux, g mole/sq cm sec, or Avogadro's number, or integer in Eq. (38)
- r_c = critical radius of two -dimensional nucleus, cm
- R = gas constant, cal/g mole °K, or ratio of interfacial rate constants for species A and B
- s = interference fringe spacing, mm
- S = molar entropy, cal/g mole °K

t = thickness of optical wedge at observation point, mm.
T = temperature, °C or °K.
u = average molecular velocity, cm/sec.
v = specific volume, cc/g.
V = freezing velocity, cm/sec, or molar volume, cc/g mole.
x = mole fraction in solid phase
y = mole fraction in liquid phase

GREEK LETTERS

α = angle, degree
 β = separation factor, or angle, degree
 Γ = solid phase activity coefficient
 γ = liquid phase activity coefficient
 η = viscosity, poise
 λ = interatomic spacing, cm.
 λ_0 = wavelength, 6328 Å, for He-Ne gas laser
 μ = chemical potential, cal/g mole
 ρ = molar density, g mole/cc
 σ = interfacial surface free energy, cal/sq cm
 χ = transmission coefficient
 ω = excess free energy, cal/g mole

SUPERSCRIPTS

F = forward process
L = liquid state property
O = standard state property
R = reverse process

- S = solid state property
- ‡ = activated state property
- * = equilibrium condition

SUBSCRIPTS

- A = component A, minor component, bibenzyl
- B = component B, major component, stilbene
- C = crystallization activated state property
- e = equilibrium condition
- ex = experimental condition
- f = fusion process
- i = interfacial condition
- L = liquid state property
- m = melting process
- O = initial condition
- S = solid state property
- T = constant temperature condition
- V = viscous flow activated state property

LITERATURE CITED

- Bondi, A., J. Chem. Phys. 14, 591 (1936).
- Burton, W., Cabrera, N., and Frank, F. C., Phil Trans. Roy. Soc. A243, 299 (1951).
- Cahn, J., Hillig, W., and Sears, G., Acta Meta. 12, 1421 (1964).
- Chalmers, B., "Principles of Solidification", J. Wiley and Sons, New York (1964).
- Cheng, C. T., and Pigford, R. L., Paper submitted for publication.
- Cheng, C. T., Ph.D. Thesis, Chem. Eng. Dept., University of California (1969).
- Chernov, A. A., "The Spiral Growth of Crystals", Soviet Physics Uspekhi. 4, 116 (1961).
- Clifton, D., Ph.D. Thesis, University of Utah (1957).
- Frank, F. C., Disc. Farad. Soc. 5, 48 (1948).
- Glasston, S., Laidler, K., and Eyring, H., "Theory of Rate Processes", McGraw-Hill, New York (1941).
- Hillig, W. B., and Turnbull, D., J. Chem. Phys. 12, 914 (1956).
- Jackson, K. A., Uhlmann, D. R., and Hunt, J. D., J. Crystal Growth 1, 1 (1967).
- Jackson, K. A., in "Growth and Perfection of Crystals", J. Wiley and Sons, New York (1958).
- Jackson, K. A., "A Review of the Fundamental Aspects of Crystal Growth" in "Crystal Growth", Pergamon, Oxford (1967).
- Jackson, K. A., "Current Concepts in Crystal Growth from the Melt" in "Progress in Solid State Chemistry" Vol. IV, (1967).

- Kirwan, D. J., and Pigford, R. L., A.I.Ch.E.J. 15, 442 (1969).
- Kirwan, D. J., Ph.D. Thesis, Chem. Eng. Dept., University of Delaware (1967).
- Kolosov, N. Ia., Soviet Physics-Crystallography 3, 707 (1958).
- Turnbull, D., in "Solid State Physics", Vol. III, Academic Press, New York (1958).
- Van Hook, A., "Crystallization", Rheinhold Publ. Co., New York (1963).
- Vignes, A., Ind. Eng. Chem. Fund. 5, 189 (1966).
- Whitaker, S., and Pigford, R. L., Ind. Eng. Chem. 50, 1026 (1958).
- Wilke, C. R., and Chang, P., A.I.Ch.E.J. 1, 264 (1955).

LEGAL NOTICE

This report was prepared as an account of Government sponsored work. Neither the United States, nor the Commission, nor any person acting on behalf of the Commission:

- A. Makes any warranty or representation, expressed or implied, with respect to the accuracy, completeness, or usefulness of the information contained in this report, or that the use of any information, apparatus, method, or process disclosed in this report may not infringe privately owned rights; or*
- B. Assumes any liabilities with respect to the use of, or for damages resulting from the use of any information, apparatus, method, or process disclosed in this report.*

As used in the above, "person acting on behalf of the Commission" includes any employee or contractor of the Commission, or employee of such contractor, to the extent that such employee or contractor of the Commission, or employee of such contractor prepares, disseminates, or provides access to, any information pursuant to his employment or contract with the Commission, or his employment with such contractor.

TECHNICAL INFORMATION DIVISION
LAWRENCE RADIATION LABORATORY
UNIVERSITY OF CALIFORNIA
BERKELEY, CALIFORNIA 94720